NeuroImage: Clinical 7 (2015) 667–677

Contents lists available at ScienceDirect

NeuroImage: Clinical

journal homepage: www.elsevier.com/locate/ynicl

Fibromyalgia is characterized by altered frontal and cerebellar structural covariance brain networks

Hyungjun Kim[a,b,*], Jieun Kim[a,b], Marco L. Loggia[a], Christine Cahalan[c], Ronald G. Garcia[a,d], Mark G. Vangel[a], Ajay D. Wasan[e], Robert R. Edwards[c,1], Vitaly Napadow[a,c,f,1]

[a]Athinoula A. Martinos Center for Biomedical Imaging, Massachusetts General Hospital, Harvard Medical School, Charlestown, MA 02129, USA
[b]Division of Medical Research, Korea Institute of Oriental Medicine, Daejeon 305-811, South Korea
[c]Department of Anesthesiology, Perioperative and Pain Medicine, Brigham and Women's Hospital, Harvard Medical School (HMS), Chestnut Hill, MA 02467, USA
[d]School of Medicine, Universidad de Santander, Bucaramanga, Colombia
[e]Departments of Anesthesiology and Psychiatry, University of Pittsburgh School of Medicine, Pittsburgh, PA 15261, USA
[f]Department of Biomedical Engineering, College of Electronics and Information, Kyung Hee University, Yongin, 449-701, South Korea

ARTICLE INFO

Article history:
Received 24 December 2014
Received in revised form 24 February 2015
Accepted 27 February 2015
Available online 4 March 2015

Keywords:
Fibromyalgia
Pain
Network
Tractography
Cerebellum

ABSTRACT

Altered brain morphometry has been widely acknowledged in chronic pain, and recent studies have implicated altered network dynamics, as opposed to properties of individual brain regions, in supporting persistent pain. Structural covariance analysis determines the inter-regional association in morphological metrics, such as gray matter volume, and such structural associations may be altered in chronic pain. In this study, voxel-based morphometry structural covariance networks were compared between fibromyalgia patients ($N = 42$) and age- and sex-matched pain-free adults ($N = 63$). We investigated network topology using spectral partitioning, which can delineate local network submodules with consistent structural covariance. We also explored white matter connectivity between regions comprising these submodules and evaluated the association between probabilistic white matter tractography and pain-relevant clinical metrics. Our structural covariance network analysis noted more connections within the cerebellum for fibromyalgia patients, and more connections in the frontal lobe for healthy controls. For fibromyalgia patients, spectral partitioning identified a distinct submodule with cerebellar connections to medial prefrontal and temporal and right inferior parietal lobes, whose gray matter volume was associated with the severity of depression in these patients. Volume for a submodule encompassing lateral orbitofrontal, inferior frontal, postcentral, lateral temporal, and insular cortices was correlated with evoked pain sensitivity. Additionally, the number of white matter fibers between specific submodule regions was also associated with measures of evoked pain sensitivity and clinical pain interference. Hence, altered gray and white matter morphometry in cerebellar and frontal cortical regions may contribute to, or result from, pain-relevant dysfunction in chronic pain patients.

1. Introduction

Advances in non-invasive structural neuroimaging, including voxel-based morphometry (VBM), diffusion tensor imaging (DTI), and surface-based cortical thickness analyses, have been used to investigate altered brain structure associated with multiple clinical disorders. Anatomical brain changes in chronic pain patients have now been reported by multiple studies, and a recent voxel based morphometry meta-analysis including 23 publications and close to 500 chronic pain patients found reduced gray matter volume in the basal ganglia, thalamus, anterior and posterior insula, anterior cingulate and both medial and lateral prefrontal cortices (Smallwood et al., 2013). Increased gray matter volume was also noted in the striatum and cerebellum (Schmidt-Wilcke et al., 2007).

Network analysis to evaluate inter-regional connectivity in the human brain has been performed with both functional and structural neuroimaging data (Bullmore and Sporns, 2009). Structural covariance analysis determines the inter-regional association in morphological metrics, such as gray matter volume. Specifically, this form

Abbreviations: AAL, automated anatomical labeling; BDI, Beck depression inventory; BPI, brief pain inventory; DTI, diffusion tensor imaging; FM, fibromyalgia; fMRI, functional MRI; FSL, FMRIB software library; HC, healthy controls; MCP, middle cerebellar peduncle; MNI, Montreal neurological institute; MRI, magnetic resonance imaging; ROI, region of interest; SCP, superior cerebellar peduncle; SPM, statistical parametric mapping; P40, the pressure level (mm Hg) for a pain intensity rating of 40/100; VBM, voxel-based morphometry.

* Corresponding author at: Martinos Center for Biomedical Imaging, Building 149, Suite 2301, Charlestown, MA 02129, USA. Fax: +1 617 726 7422.
E-mail address: hengjun@nmr.mgh.harvard.edu (H. Kim).

[1] These authors contributed equally to this work.

http://dx.doi.org/10.1016/j.nicl.2015.02.022

of network-based analysis determines how gray-matter volume in a given brain region covaries with that of other brain regions, across large multi-subject datasets (Evans, 2013). In healthy adults, the covariance network has been found to exhibit small world properties (i.e. nodes have more local connections than that of a random network) (He et al., 2007), similar to functional connectivity network topology (Bullmore and Sporns, 2009), and strong covariance has been found for homotopic regions across hemispheres (Mechelli et al., 2005). Such covariance likely arises from a combination of genetic influences during development and aging, as well as environmental/behavioral factors known to produce experience-based neuroplasticity. As such, chronic pain perception may also play an important role in shaping structural covariance in the human brain.

Brain structural covariance analysis has been performed for several pain disorders such as migraine (Liu et al., 2012) chronic back pain, knee osteoarthritis, and complex regional pain syndrome (Baliki et al., 2011), but not fibromyalgia (FM). Moreover, prior structural covariance analyses did not investigate if alterations in gray matter volume covariance were accompanied by altered white matter connectivity. Chronic pain, widely distributed throughout the body, is a key symptom of patients suffering from FM (Clauw, 2014). This functional pain disorder is characterized by altered resting functional connectivity (Napadow et al., 2010), which is associated with spontaneous pain intensity, and which can be normalized following longitudinal therapy (Harris et al., 2013; Napadow et al., 2012). FM also exhibits decreased gray matter volume in the medial frontal gyri (Kuchinad et al., 2007) and increased gray matter volume in cerebellum (Schmidt-Wilcke et al., 2007), as evidenced by VBM. Altered white matter microstructure in FM has been noted with DTI in the thalamus and postcentral gyrus (Lutz et al., 2008). Hence, we hypothesized that this centralized, functional pain syndrome may also demonstrate altered structural network topology, and white matter connectivity, specifically associated with clinically-relevant pain outcome measures.

In this study, fibromyalgia patients and age- and sex-matched, pain-free adults were enrolled in a structural covariance analysis. The aim of this study was three-fold. First, we compared structural covariance networks, including cerebral and cerebellar structures, in FM patients with those in healthy controls. Second, we investigated network topology using spectral partitioning, which can delineate local network submodules specific to FM. Third, we explored white matter connectivity within these submodules, using DTI, and evaluated the association between pain severity and the strength of structural connectivity using probabilistic tractography. Our study provides a detailed analysis of brain structural connectomics in FM patients suffering from chronic pain.

2. Materials and methods

2.1. Participants

We recruited 43 patients with fibromyalgia and 63 healthy controls (HC). Each subject provided written, informed consent in accordance with the Human Research Committee of Partners Health Care and Massachusetts General Hospital. The diagnosis of fibromyalgia was confirmed by physician and medical records, and patients also met the recently-proposed Wolfe et al. criteria (Wolfe et al., 2010), which require the presence of widespread pain as well as the endorsement of a number of somatic and cognitive symptoms. All participants underwent medical evaluations to exclude current or previous disorders that could affect brain structure. The exclusion criteria for FM subjects were as follows: (1) concurrent autoimmune or inflammatory disease that causes pain, such as rheumatoid arthritis, systemic lupus erythematosus, or inflammatory bowel disease; (2) a history of significant neurologic disorders, cardiovascular disorders, psychotic disorders, or cognitive impairment preventing completion of study procedures; (3) a history of drug abuse; (4) a history of head trauma requiring medical attention; and (5) brains with significant structural abnormality, which were referred to neuroradiological review. For healthy controls, subjects met the exclusion criteria above and were devoid of pain.

2.2. Clinical and behavioral measures for FM

Evoked pain sensitivity was measured in FM using cuff pain algometry applied to the left lower leg, over the gastrocnemius muscle belly. This mode of pressure pain algometry was used as it preferentially stimulates deep tissue nociceptors (Polianskis et al., 2002). As most clinical pain originates in deep tissue rather than cutaneous receptors, the investigation of brain responses to deep tissue pain may be more clinically relevant than brain responses to evoked cutaneous (e.g. heat) pain (Kim et al., 2015; Loggia et al., 2014; Polianskis et al., 2002). Briefly, pain stimuli were delivered with a velcro-adjusted pressure cuff connected to a rapid cuff inflator, which inflated the cuff to a constant pressure level (Hokanson Inc., Bellevenue, WA, USA). Quantitative sensory testing began by inflating the cuff to 60 mm Hg of pressure, and the level of pressure was adjusted in 10 mm Hg increments or decrements until a pain intensity rating of 40/100 was obtained. This pressure level, in mm Hg, was referred to as P40, and has been shown to be lower in FM patients than controls, reflecting the global hyperalgesia that characterizes this condition (Loggia et al., 2014). This procedure has also been described in more detail elsewhere (Kim et al., 2013; Loggia et al., 2014).

Patients completed the brief pain inventory (BPI) (Cleeland, 1991) and Beck depression inventory (BDI) (Beck et al., 1961) to evaluate their clinical pain and psychosocial functioning.

2.3. MRI acquisition

Structural MRI scans were obtained on a 3.0 T Siemens Trio (Siemens Medical, Erlangen, Germany) equipped with 32-channel head coil at the Athinoula A. Martinos Center for Biomedical Imaging, Massachusetts General Hospital. T1-weighted sagittal volumes were obtained using a three-dimensional (3D) MPRAGE pulse sequence with the following parameters: 1.64 ms echo time (TE), 2530 ms repetition time (TR), 7° flip angle (FA), 1200 ms inversion time (TI), and $1 \times 1 \times 1$ mm^3 spatial resolution. Diffusion-weighted images were also obtained using spin-echo echo-planar imaging (EPI) sequence with the following parameters: 84 ms echo time (TE), 8040 ms repetition time (TR), 2 mm slice thickness, and 2 mm in-plane resolution. The diffusion-sensitizing gradients with a b-value of 700 s/mm^2 were applied to the 60 non-collinear directions, and 10 volumes with no diffusion weighting were also acquired.

One patient was excluded due to the presence of motion artifact on the T1-weighted image volume. Thus, 105 images were used for structural covariance analysis. For tractography analysis, diffusion-weighted image volumes of 39 healthy controls and 30 patients were available.

2.4. Segmentation and registration

Brain gray matter segmentation and alignment were performed using the VBM8 toolbox (http://dbm.neuro.uni-jena.de/vbm) as implemented in SPM8 (Statistical Parametric Mapping, http://www.fil.ion.ucl.ac.uk/spm/) (Ashburner and Friston, 2005), which included the field inhomogeneity correction, skull stripping, probabilistic tissue classification of gray matter, white matter, and cerebrospinal fluid, nonlinear registration to standard space using DARTEL (Ashburner, 2007), and intensity modulation by the Jacobian determinant. DARTEL uses a non-linear algorithm to yield excellent co-registration results, in terms of overlap and distance measures, for VBM analysis (Klein et al., 2009). The intracranial volume was calculated by summing the volumes of the segmented gray matter, white matter, and cerebrospinal fluid compartments, which was used as nuisance variable in the following correlational analyses.

2.5. Structural covariance analysis

Regional gray matter volume of 101 ROIs including cerebral cortices (78 ROIs) and cerebellum (23 ROIs) were estimated with VBM8 using the mean value from the segmented gray matter image and automated anatomical labeling (AAL) atlas (Tzourio-Mazoyer et al., 2002). In this atlas, parcellation of cerebral cortices was mainly based on developmentally consistent brain sulci, primary and secondary sulci, which first appear during fetal development (Chi et al., 1977). Cerebellar parcellation of the AAL atlas was based on previous work by Schmahmann et al. (1999). For accurate measurement, the AAL atlas (which is based on the Colin-27 atlas) was aligned to the averaged brain image obtained from all 105 subjects (which were originally aligned to Montreal neurological institute (MNI) space). The cerebellar flocculonodular lobe was excluded in our network analyses because of its variable location and small volume.

Structural covariance analysis for the FM and HC groups was then performed. Using data from 63 controls and 42 FM patients, group-level partial correlation coefficients for volumes of 101 ROIs were calculated after controlling for age, sex, and intracranial volume, which yielded two symmetric matrices with 101 by 101 cells. In a previous study, this type of VBM-based structural covariance analysis successfully differentiated a preterm adolescents-related covariance pattern for connections between cerebral cortex and cerebellum (Nosarti et al., 2011). Each matrix contained coefficients for 5050 ($=101 \times 100 / 2$) possible pairs using the 101 individual parcellation ROIs. We then compared FM and HC matrices by contrasting the strength of associations within each lobe and cerebellum for both hemispheres. Correlation coefficients in FM and HC matrices were contrasted using the asymptotic χ^2-test (Jennrich, 1970), and *R* (version 2.5.0, R Foundation for Statistical Computing) as follows:

$$\chi^2 = \sum_{i=1}^{2}\left(\frac{1}{2}tr\left(Z_i^2\right) - dg'\left(Z_i'\right)S^{-1}dg(Z_i)\right)$$

$$\bar{R} = \frac{(n_1R_1 + n_2R_2)}{n_1 + n_2} = (\bar{r_{ij}})$$

$$S = \left(\delta_{ij} = \overline{r_{ij}r^{ij}}\right)$$

$$\delta_{ij} = Kronecker's\ delta$$

$$Z_i = \sqrt{n_i}\bar{R}^{-1}(R_j - \bar{R})$$

where for $i = 1$ to 2; R_i are the correlation matrix for $p \times p$ elements obtained from sample size n_i data; χ^2 distribution with the degree of freedom $= p \times (p - 1) / 2$. Finally, effect sizes (Cohen's *d*) are also reported for these differences.

As the number and volume of ROIs may influence structural connectivity networks (Hagmann et al., 2008), we also repeated the structural covariance analysis using 531 ROIs. These were formed by dividing the AAL ROIs into 531 ROIs with the similar volume (approximately 2.5 cm^3), where the borders aligned with those of AAL ROIs (Supplementary Fig. 1). As such, we increased the number of parcellations to test the dependency of our observation on the number of ROIs.

2.6. Binarization for network analysis

In order to identify structural covariance networks based on morphological measures, we utilized the simple binarization of the matrix to obtain the adjacency matrix, *G* (Bassett et al., 2008; He et al., 2008). This matrix represents an undirected graph with *N* nodes (i.e. 101 ROIs) and *K* edges. The edge K_{ij} represents the connection between two nodes, *i* and *j*, and is set to either a value of 1 or 0. The edge is defined as 'connected' (and assigned a value of 1), if the correlation coefficient between the two nodes is greater than a specific threshold. In our study, this threshold was defined by utilizing the concept of sparsity, as clarified below. The correlation matrix for each group contains different coefficients in their matrix. If the same correlation coefficient threshold were selected for both groups (FM and HC), the resulting matrix *G* would have different numbers of edges. Consequently, differences between groups for network-based metrics may not reflect true topological changes in the constituent networks (He et al., 2008). To minimize potential bias, we used sparsity-based thresholding, where sparsity is defined as the total number of edges in a network divided by the maximum possible number of edges (He et al., 2008). Thus, after sparsity-based thresholding, the networks of both groups will have the same total number of connections. In the current study, the threshold was determined by a sparsity value of 0.11, which was determined by the lowest value allowing for all nodes to be fully connected (no node islands) in both healthy control and FM networks and small-world features are evident (detailed description of sparsity and small-world network properties is presented in Supplementary Material and Supplementary Fig. 2). At a sparsity of 0.11, each network has the same number ($555 = 5050 \times 0.11$) of connections, and the correlation coefficient threshold for the healthy control network was $r = 0.409$, and for FM patients was $r = 0.437$. Coincidentally, these values are very similar to a correlation coefficient threshold determined by using a false discovery rate-corrected *q* value of 0.05 for 5050 cells in the FM network matrix, which was $r = 0.436$.

2.7. Network degree analysis

Degree is a nodal metric defined by the number of significant connections of a node with the other nodes in the binarized structural covariance network matrix, *G* (Bullmore and Sporns, 2009). This means that a brain region with many connections to other ROIs in the brain will have high degree value. We computed the degrees of all nodes in each whole-brain network matrix, and calculated the differences of degrees between FM and HC for these 101 nodes (i.e. ROIs), which were then used for topological metric comparisons between groups based on permutation testing, as previously introduced by Bassett et al. (Bassett et al., 2008). In this permutation test, VBM-based regional gray matter volumes for 101 ROIs for each participant were randomly assigned to healthy controls or FM groups, resulting in each group having the same number of participants as the original assignment, but with different members. Partial correlation coefficients were calculated controlling for age, sex, and intracranial volume, and were thresholded based on the above-mentioned sparsity. Subsequently, network degrees for 101 ROIs were computed for each group and between-group differences were calculated. This procedure was repeated 10,000 times to sample the degree difference permutation distributions under the null hypothesis that network degree was not determined by original group assignment. A one-tailed *P*-value was then calculated by counting how many times the result was greater (or smaller) than the original between-group difference (Bassett et al., 2008).

2.8. Spectral partitioning analysis

Brain networks can be divided into a number of sub-modules with distinct functional features (Chen et al., 2008). To identify such submodules based on the network matrix in each group, we used spectral partitioning, which determines the number of submodules based on network topology itself, where these submodules are detected by optimizing the modularity, *Q* (Newman, 2006; Wolfe et al., 2010).

$$Q = \frac{1}{2m}\sum_{i \neq j \in G}\left(a_{i,j} - \frac{k_ik_j}{2m}\right)\delta(M_i, M_j)$$

where m is the number of edges, a is the adjacency matrix of the graph G, M_i is the module containing node i, and $\delta(M_i, M_j) = 1$ if $M_i = M_j$, and 0 otherwise.

Using this modularity estimation, the structural covariance network was subdivided into covariance-based sub-modules, defined by rich connections within a submodule, and sparse connections between submodules (Newman, 2006).

We further explored associations between total submodule volume and clinical variables relevant to core fibromyalgia symptomatology. Correlation analyses were conducted between submodule volume and (1) evoked pain sensitivity (i.e. cuff pressure at P40), (2) BPI, (3) BDI, and (4) disease duration, where the submodule volumes were adjusted for age, sex, and intracranial volume.

2.9. DTI tractography

In addition to VBM-based network analyses, DTI data were also used to assess structural connectivity differences between FM and HC. This analysis was focused on white matter tractography within submodules identified with the spectral partitioning method described above. All diffusion image preprocessing was conducted using the Functional MRI of the Brain (FMRIB) software library (FSL, http://www.fmrib.ox.ac.uk/fsl). Fiber tracts were estimated using Bayesian Estimation of Diffusion Parameters Obtained using Sampling Techniques (BedpostX) (Behrens et al., 2003) with a model allowing for crossing fibers, which produces more reliable results compared to a single-fiber model (Behrens et al., 2007). As a previous study reported that results ceased to differ from upwards of 750 samples (Ramnani et al., 2006), we conservatively conducted tractography analysis using 1000 samples. At each voxel within seed regions, we initiated 1000 tract-following samples, resulting in a probabilistic map of connectivity. Tractography was conducted in each subject's native space, and probabilistic maps were then warped into MNI standard space for cross-subject averaging and comparison using FMRIB's Nonlinear Image Registration Tool (FNIRT) (Woolrich et al., 2009).

The seed and target clusters for tractography analysis were determined based on the results of spectral partitioning, which showed that FM brain regions can be divided into 4 distinct structural covariance submodules. We found that the volumes of 2 submodules were significantly associated with clinical measures (see Results). Briefly, one such submodule comprised 4 clusters including medial prefrontal/orbitofrontal cortex, medial temporal lobe, right inferior parietal lobule, and cerebellum, and was referred to as the submodule 1. The other submodule comprised 3 clusters including lateral orbitofrontal cortex, lateral temporal lobe, and insula, and was referred to as the submodule 2. Tractography analyses were performed for each of these submodules, in each hemisphere.

Seed and target clusters for fiber-tracking of cortico-cortical connections were located at gray-white matter boundaries for the AAL ROIs characterizing distinct clusters in the submodules. As seed clusters were determined based on the covariance of gray matter volume, we chose the white matter border adjacent to the gray matter of regions of interest as tracking starting points (Kloppel et al., 2008; Tomassini et al., 2007). Thus, the boundary was defined by voxels comprised by both >30% gray matter and >30% white matter density. Gray and white matter densities were calculated from the average gray and white matter maps of all 105 subjects. We focused our cortico-cortical tractography analysis on intra-hemispheric connections, while tracts passing through the thalamus were excluded to avoid interference from corticothalamic projections (Ford et al., 2010). For tractography analyses between cortical and cerebellar cluster, the target mask was placed on the cerebellar part of the middle cerebellar peduncle, which is known to carry afferents to the cerebellum. To avoid erroneous tracking, the exclusion mask was delineated around the cerebellar tentorium (Supplementary Fig. 3). Previous studies have demonstrated the existence of bilateral cerebellar projections from right and left red and pontine nuclei (Brodal, 1979; Mower et al., 1980). Thus, bilateral masks for middle cerebellar peduncle (MCP) were used in this analysis. Superior cerebellar peduncle (SCP)-based tracts were excluded from this tractography analysis because not all subjects showed successful connectivity to the SCP target mask from bilateral medial orbitofrontal cortex, bilateral medial temporal lobe and right inferior parietal lobule. Inferior cerebellar tracts to/from the medulla were also excluded from this analysis because its low density, divergent topology, and inferior location with more variable MRI signal-to-noise ratio may introduce estimation bias (Habas and Cabanis, 2007). For analyses between medial orbitofrontal cortex and cerebellar seeds, tractography was not successful in some subjects, that is, the tracts of some participants did not reach the MCP mask. Thus, we excluded this specific tract from the MCP-based analysis. Previous animal studies have shown a lack of evidence for tracts connecting ventral prefrontal areas to pontine nuclei (Schmahmann, 1996), possibly explaining the unsuccessful tractography results for this tract. In summary, we conducted tractography analyses for tracts where all subjects successfully reached the target mask. For the submodule 1, there were 5 tracts tested (medial orbitofrontal cortex to medial temporal lobe, bilateral; right medial temporal lobe to cerebellum, right inferior parietal lobule to medial temporal lobe, right inferior parietal lobule to cerebellum). For the submodule 2, there were also 6 tracts tested (insula to lateral temporal lobe, bilateral; insula to lateral orbitofrontal cortex, bilateral; lateral orbitofrontal cortex to lateral temporal lobe, bilateral). The results of the tractography analysis are shown in Supplementary Fig. 3.

We estimated white matter connectivity by the number of fibers determined from probabilistic tractography. For DTI-based analyses, we first performed a logarithmic transformation on the numbers of fibers calculated, in order to remove skewness. To explore the association between structural connectivity and clinical variables, correlation analyses were conducted between the numbers of fibers connecting seed and target clusters and clinical pain-related measures. In these correlation analyses, the numbers of fibers were adjusted for age and sex.

For parametric testing all data were first tested for adherence to a normal distribution assessed by the Kolmogorov–Smirnov test. All the statistical tests except the asymptotic χ^2-test were performed using the Statistical Package for Social Sciences (SPSS 17.0; SPSS Inc., Chicago, IL).

3. Results

There were no significant differences between fibromyalgia patients and healthy control groups in sex distribution (FM: 85.7% female; HC: 76.2% female), age (years, FM: 45.3 [mean] ± 11.6 [SD]; HC: 42.8 ± 13.7), or intracranial volume (cc, FM: 1350 ± 116; HC: 1368 ± 121). FM patients reported moderate levels of pain (BPI severity = 5.5 ± 2.0; BPI interference = 5.7 ± 2.2) and depression symptomatology (BDI, FM: 15.0 ± 9.1; HC: 3.1 ± 3.9). Evoked pain sensitivity was assessed by cuff algometry and demonstrated a range of sensitivity over our cohort (pressure to elicit 40/100 pain (P40), mm Hg, FM: 102 ± 55; HC: 191 ± 86). BDI and evoked pain sensitivity were assessed in a subset ($n = 15$) of the healthy controls that contributed brain-based data to our analysis. While not the focus of this study, BDI was generally higher in FM compared to HC (t-test, $P < 0.0001$) and FM patients were also more sensitive to evoked cuff pain compared to HC (t-test, $P = 0.001$) (see Table 1). There was no correlation between BDI and pain sensitivity in FM patients ($r = 0.01$, $P = 0.94$).

Structural T1-weighted MRI datasets were used to calculate gray matter volume through VBM. VBM values were averaged within 101 distinct cerebral and cerebellar ROIs in each individual and were used to calculate a group-wise structural covariance matrix for both FM and HC groups (Fig. 1). We compared the association strength across bilateral cerebellar ROIs between groups, and found that correlation coefficients in FM patients were significantly higher than controls ($P = 0.0025$; Cohen's d, 0.49). In contrast, association strength across frontal lobe ROIs was decreased (lower correlation coefficients) in FM compared to healthy adults

Table 1
Demographic and clinical data for fibromyalgia patients and controls.

	Patients ($N = 42$)	Controls ($N = 63$)	P-value
Sex (F/M)	36/6	48/15	0.32
Age (years)	45.3 (11.6)	42.8 (13.7)	0.32
Intracranial volume (cm^3)	1350 (116)	1368 (121)	0.44
BDI (0–63)[a]	15.0 (9.1)	3.1 (3.9)	<0.0001
Evoked pain sensitivity (P40 pressure, mm Hg)[a]	102 (55)	191 (86)	0.001
BPI severity (0–10)	5.5 (2.0)	–	–
BPI interference (0–10)	5.7 (2.2)	–	–
Disease duration (years)[b]	13.9 (11.6)		

Age, intracranial volume, BDI, and evoked pain sensitivity are presented as mean (SD), and compared between groups using an independent Student's t-test. Sex distribution was compared using a Fisher's exact test. Abbreviations: BDI, Beck depression inventory; BPI, brief pain inventory.

[a] These clinical metrics were assessed in a subset ($N = 15$) of the healthy controls.

[b] These clinical metrics were assessed in a subset ($N = 33$) of the fibromyalgia patients.

($P = 0.0002$; Cohen's d, 0.60). No differences were found between groups *within* the parietal, occipital, and temporal lobes after Bonferroni correction.

We repeated this analysis using 531 ROIs, which gave a similar result (Supplementary Fig. 4). Specifically, correlation coefficients in FM patients were significantly higher than in controls across cerebellar ROIs ($P = 0.0005$) while the association strength across frontal lobe ROIs was decreased in FM compared to healthy adults ($P < 0.0001$).

Using a sparsity threshold of 0.11 (see Supplementary Fig. 2), we performed a topological network analysis by first visualizing a binary undirected network matrix for FM and HC groups, separately, where higher correlations between ROI nodes were displayed by edges (Fig. 2). We found evidence of small-world properties for both FM and HC networks, using the delta scalar parameter ($\delta = 3.8$, 4.3 for FM and HC, respectively, at sparsity = 0.11), which determines small-worldness at $\delta \gg 1$, consistent with previous studies (Bassett et al., 2008; He et al., 2008). While the healthy control network demonstrated dense connections within the frontal lobe, the FM network demonstrated dense connections within the cerebellum. In addition, FM demonstrated connections between cerebellum and right inferior parietal lobule, bilateral parahippocampal gyri, and bilateral medial prefrontal/orbitofrontal cortex. As mentioned above, we repeated the analysis using 531 ROIs, which also showed that healthy controls demonstrated dense connections within the frontal lobe, while the FM network demonstrated dense connections within the cerebellum (Supplementary Fig. 5).

Degree, or sum of connections for any given ROI, is a fundamental network parameter (Bullmore and Sporns, 2009) and can be used to compare network topology between groups. We found that cerebellar ROIs, such as Crus I, lobule IV/V and VI, showed significantly greater degree for FM compared to HC (Table 2). This was also the case for right inferior parietal lobule, and supramarginal gyrus, and left parahippocampal gyrus. These ROIs showed connections with other brain regions including prominent cerebellar ROIs in the FM network (Fig. 2B). On the other hand, HC demonstrated greater degree for the right postcentral gyrus and gyrus rectus, and the left medial orbital frontal gyrus, and inferior frontal opercular gyrus (Table 2). These regions showed connections to other brain regions including multiple prefrontal ROIs in the HC network (Fig. 2B).

Subsequently, we conducted spectral partitioning based on the binarized structural covariance network, which successfully divided the 101 ROIs into several submodules (Fig. 3). For the HC network, modularity was optimized with 5 submodules ($Q = 0.523$), while for the FM network, modularity was optimized with 4 submodules ($Q = 0.443$). In the control network, a submodule was comprised by all cerebellar ROIs, indicating greater covariance within cerebellar ROI volumes, and not between cerebellar and cerebral ROIs. In the FM network, the "cerebellar" submodule included cerebellar ROIs in addition to bilateral medial prefrontal/orbitofrontal cortex, bilateral medial temporal lobe, and right inferior parietal lobule. This was referred to as *submodule 1*. Specifically, this submodule comprised AAL ROIs labeled right inferior parietal lobule, supramarginal gyrus, superior medial frontal gyrus, left lingual gyrus, bilateral parahippocampal gyrus, fusiform gyrus, medial orbital frontal gyrus, and gyrus rectus.

In the HC network, the frontal lobe was divided into 3 submodules comprising dorsal, ventral, and cingulate subdivisions. The dorsal submodule covered superior and middle frontal gyrus and precentral gyrus, while the ventral submodule covered the orbitofrontal cortex, and stretched to the insula, superior temporal cortex, and temporal pole. In the FM network, the dorsal and cingulate submodules were merged into a single submodule, which also included the precuneus. The ventral submodule in the HC network was instead divided and merged into two submodules in FM: *submodule 2*, which included the lateral orbitofrontal cortex, lateral temporal lobe, postcentral gyrus (primary somatosensory cortex, S1), and insula, and the previously described *submodule 1*, which included the medial prefrontal/orbitofrontal cortex, medial temporal lobe, right inferior parietal lobule, and the cerebellum.

In sum, visual inspection revealed descriptively different spectral partitioning of topological network features between the two groups. Thus, we next examined the clinical relevance of these differential submodules using exploratory correlation analyses to calculate the association between submodule gray matter volume and clinical metrics in FM (i.e. evoked P40 pain sensitivity, BPI, BDI, and disease duration). We found that submodule 2 volume was correlated with evoked deep-tissue pain sensitivity (i.e. P40 pressure; $r = 0.34$; $P = 0.03$) and disease duration ($r = 0.42$; $P = 0.01$), while submodule 1 volume was correlated with BDI ($r = 0.33$; $P = 0.04$) and disease duration ($r =$

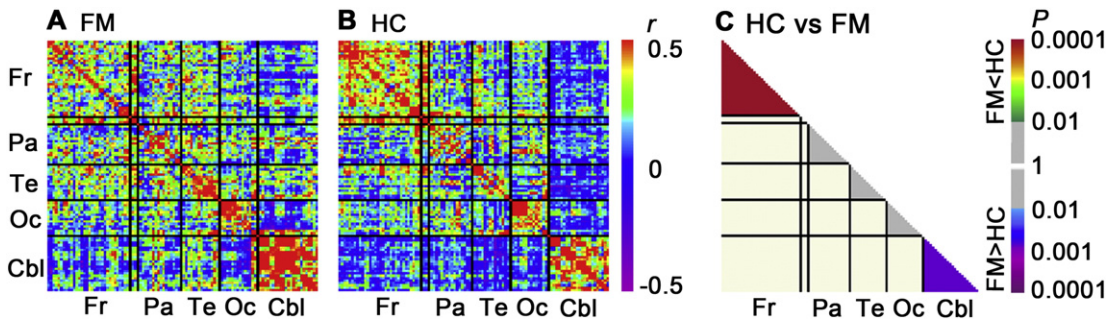

Fig. 1. Brain structural covariance matrices for fibromyalgia patients and healthy controls. Inter-regional correlation coefficients were calculated using voxel based morphometry (VBM)-derived gray matter volumes from 101 whole brain ROIs for fibromyalgia patients (A) and healthy controls (B). These partial correlations were conducted after controlling for age, sex, and intracranial volume. FM patients demonstrated greater correlation in the cerebellum (asymptotic χ^2-test, $P = 0.0025$), while healthy controls demonstrated greater correlation in the frontal lobe ($P = 0.0002$) (C). Abbreviations: Cbl, Cerebellum; Fr, frontal lobe; Oc, occipital lobe; Pa, parietal lobe; Te, temporal lobe.

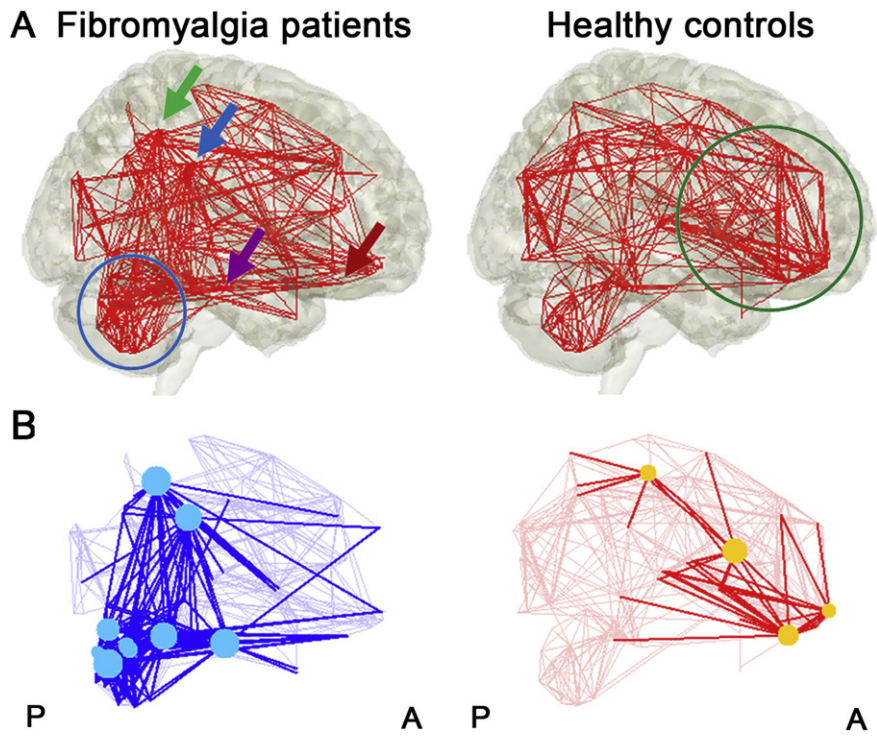

Fig. 2. Structural covariance network visualization. (A) The brain structural covariance network is visualized for both fibromyalgia patients and healthy controls. Inter-regional correlation coefficients greater than the sparsity-based threshold value are shown connected by a red line. In fibromyalgia patients, dense connections were noted within the cerebellum (blue circle). In healthy controls, prefrontal cortical regions showed dense connectivity (green circle). In addition, FM demonstrated connections between cerebellum and right inferior parietal lobe/supramarginal gyrus (green/blue arrow), bilateral parahippocampal gyri (purple arrow), and bilateral medial orbitofrontal gyri (red arrow). (B) Network degree differences were visualized with cyan (fibromyalgia patients > healthy controls) and yellow (healthy controls > fibromyalgia patients) markers, with node connection edges highlighted.

0.41; $P = 0.02$). Submodule volumes were adjusted for age, sex, and intracranial volume (Fig. 4). Volumes of other submodules were not correlated with any clinical metrics. Before being adjusted, the raw volumes of submodules showed significant correlations with age (all r's < −0.5; all P's < 0.001) and ICV (all r's > 0.6; all P's < 0.001).

Furthermore, submodules 1 and 2 comprised 3 or 4 distinct clusters. These gray matter clusters are connected to one another by white matter tracts, and probabilistic DTI-based tractography was used to assess white matter fiber counts between regions. As an exploratory analysis, we also evaluated the association between the number of fibers and pain-relevant clinical metrics for the 5 or 6 tracts in each submodule where all FM subjects contributed fibers that reached the target mask (see Materials and methods).

While the estimated number of fibers did not differ between groups, for submodule 1, the numbers of fibers between right medial temporal lobe and cerebellum, and between right inferior parietal lobule and cerebellum were significantly correlated with evoked P40 pain sensitivity ($r = -0.42$; $P = 0.03$; $r = -0.41$; $P = 0.03$, respectively), while fiber count between right medial orbitofrontal cortex and medial temporal lobe was correlated with BPI interference ($r = 0.40$; $P = 0.03$, see Fig. 5). For submodule 2, there was no correlation between the number of fibers for any ROI pair and pain-relevant clinical metrics.

Table 2
Network degree differences between fibromyalgia patients and healthy controls.

Region		Degree for FM	Degree for HC	Difference	*P*-value
Fibromyalgia patients > healthy controls					
Cerebellum crus I	Right	23	7	16	0.0006
Parahippocampal gyrus	Left	21	3	18	0.0006
Inferior parietal lobule	Right	27	4	23	0.002
Supramarginal gyrus	Right	32	8	24	0.003
Cerebellar lobule IV/V	Right	29	11	18	0.004
Cerebellum crus I	Left	19	6	13	0.009
Cerebellar lobule IV/V	Left	28	12	16	0.01
Cerebellum vermis VI		21	4	17	0.02
Cerebellar lobule VI	Left	27	16	11	0.03
Cerebellar lobule VI	Right	25	11	14	0.03
Cerebellum vermis VII		19	7	12	0.04
Healthy controls > fibromyalgia patients					
Inferior frontal operculum	Left	1	13	−12	0.01
Rectus gyrus	Right	2	19	−17	0.02
Postcentral gyrus	Right	1	9	−8	0.03
Medial orbital frontal gyrus	Left	1	14	−13	0.04

P-values were calculated based on the permutation tests.

4. Discussion

Altered brain morphometry has been widely acknowledged in chronic pain (Smallwood et al., 2013). Morphometric analyses have spanned a broad array of techniques and while structural covariance analyses have been performed for several pain disorders including migraine (Liu et al., 2012), knee osteoarthritis, and chronic back pain (Baliki et al., 2011), such studies have not been performed for more diffuse, whole body functional pain syndromes such as fibromyalgia. Moreover, prior structural covariance analyses did not investigate if alterations in gray matter volume covariance were accompanied by altered white matter connectivity, and how such changes relate to clinically-relevant metrics of dysfunction. Our structural covariance network analysis noted more dense connections in FM patients in the cerebellum, while healthy controls exhibited more dense connections within the frontal lobe. Spectral partitioning further revealed dense cerebellar connections with medial prefrontal/orbitofrontal cortex, medial temporal lobe, and right inferior parietal lobule in FM patients. These connections were merged into a distinct submodule (submodule 1), and the gray matter volume of this submodule was associated with the severity of depression symptoms in these patients. Additionally, an exploratory analysis of white matter connectivity using probabilistic

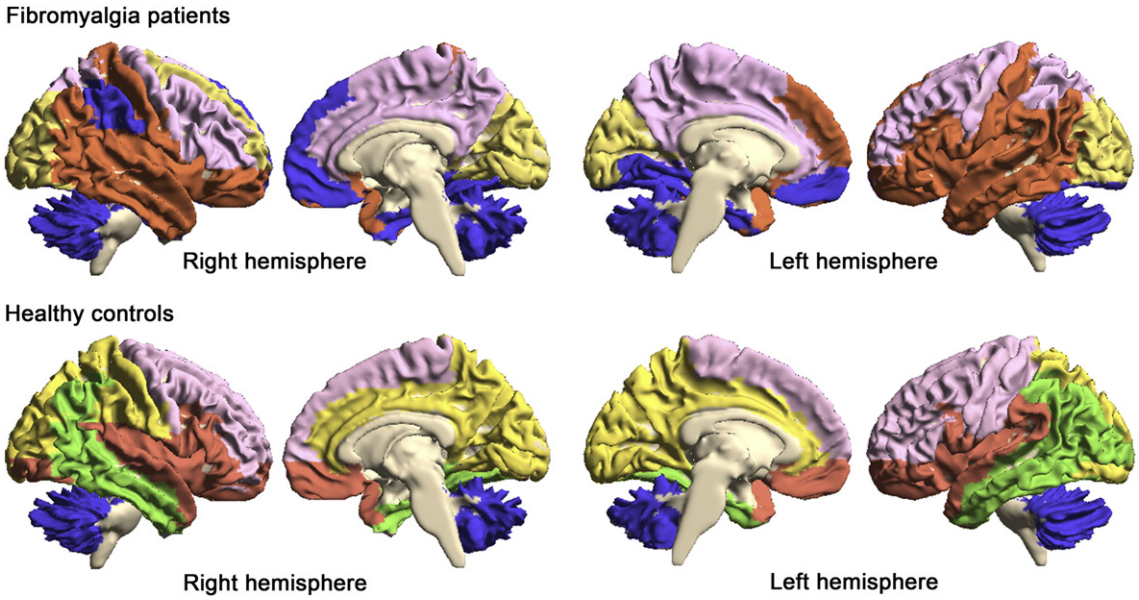

Fig. 3. Spectral partitioning submodule map. Spectral partitioning based on structural covariance effectively subdivided the brain into several distinct submodules. Of note, in healthy controls, a single submodule comprised all cerebellar ROIs, while in fibromyalgia patients, this "cerebellar" submodule (submodule 1) extended to medial prefrontal/orbitofrontal cortex, medial temporal lobe and right inferior parietal lobule (blue color).

DTI methods demonstrated that the numbers of fibers between submodule 1 regions was associated with greater evoked pain hyperalgesia and clinical pain interference. Hence, altered gray and white matter morphometry including cerebellar and frontal cortical regions may contribute to, or result from disrupted pain processing in chronic pain patients.

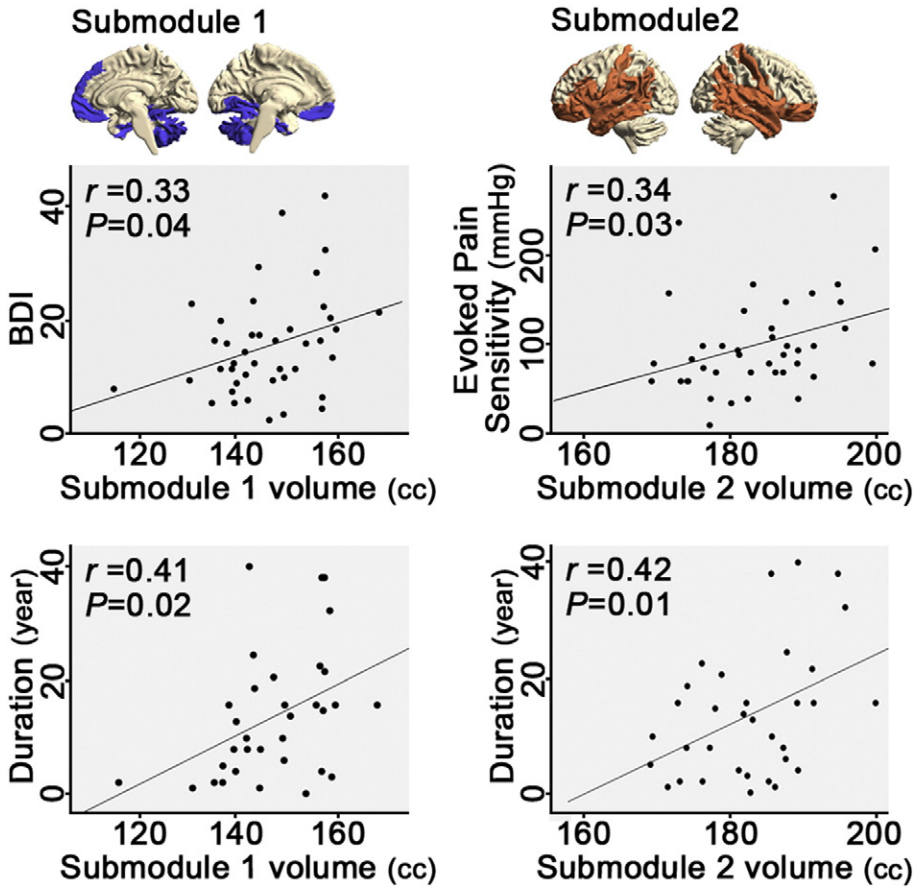

Fig. 4. Submodular gray matter volume is associated with depression, hyperalgesia, and disease duration. In fibromyalgia patients, submodule 1 (cerebellum, medial prefrontal/orbitofrontal cortex, medial temporal lobe, and right inferior parietal lobule) volume correlated with depression severity (BDI) and disease duration. Submodule 2 (lateral orbitofrontal, inferior frontal, postcentral, lateral temporal, and insular cortices) volume correlated with evoked pain sensitivity (i.e. stimulus pressure when subjects rated 40/100 pain, P40), and disease duration. Submodule 1 and 2 volumes were adjusted for age, sex and intracranial volume.

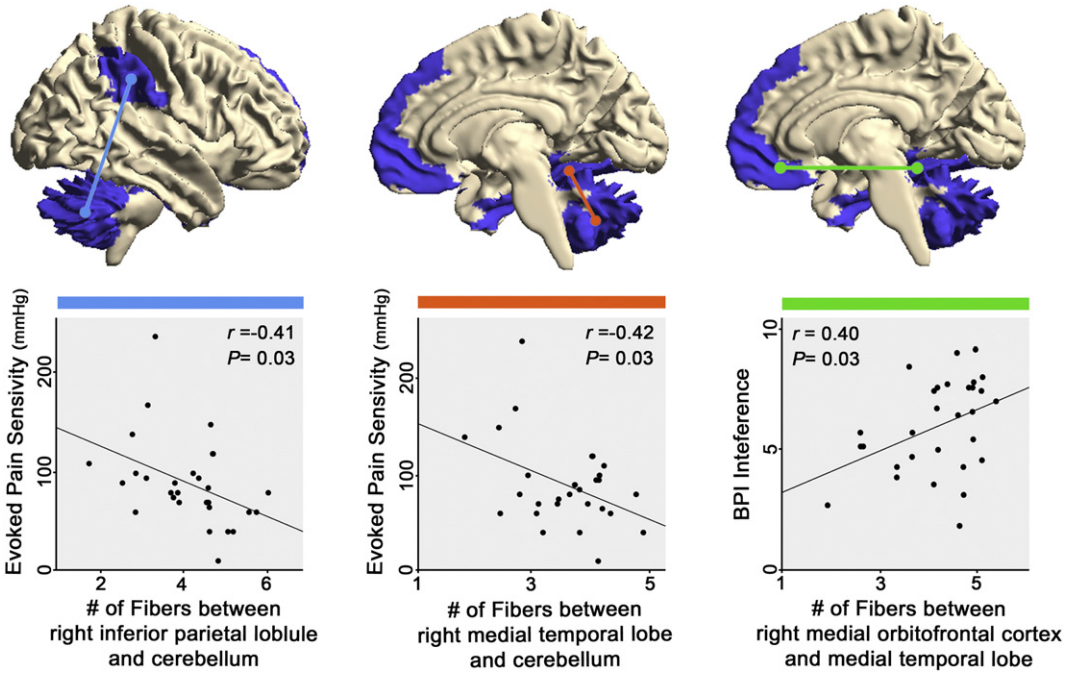

Fig. 5. White matter fiber density connecting submodule 1 regions is associated with hyperalgesia and clinical pain. Probabilistic DTI tractography was used to evaluate the number of fibers connecting component areas of submodule 1. In fibromyalgia, the number of fiber tracts estimated between cerebellum and both medial temporal lobe and inferior parietal lobule (i.e. supramarginal gyrus and secondary somatosensory cortex) was negatively correlated with evoked pain sensitivity (i.e. stimulus pressure when subjects rated 40/100 pain, P40). The number of fiber tracts between medial temporal lobe and medial orbitofrontal cortex was correlated with clinical pain interference. Number of fibers was adjusted for age and sex.

While the cerebellum is not usually thought of as a cardinal pain processing area, cerebellar involvement in nociception and chronic pain syndromes has indeed been implicated by prior research. For example, previous functional MRI studies have found that nociceptive stimuli induced cerebellar activation in lobules III to VI (Helmchen et al., 2003; Moulton et al., 2010). Our results demonstrated greater structural connectivity in lobules IV to VI for FM patients (Table 2). This topological change in the cerebellar structural covariance network may be related to the affective domain of pain processing and underlie persistent pain in this centralized pain syndrome. Moreover, in FM patients, the cerebellum did not just show rich connections between cerebellar subregions, but also between the cerebellum and cortical areas such as bilateral medial prefrontal/orbitofrontal cortex, medial temporal lobe, and right inferior parietal lobule (Fig. 2), clusters that merged into a single distinct submodule 1 (Fig. 3) by spectral partitioning.

Within submodule 1, the medial prefrontal/orbitofrontal regions demonstrated lower degree (an important network metric) in FM compared to HC subjects (Table 2 and Fig. 2B), further highlighting our finding of reduced number of edges within the FM frontal lobe. Such reduction in inter-regional covariance may be related to findings from previous VBM studies, which have noted altered gray matter volume in the frontal lobe in chronic pain (Smallwood et al., 2013). For instance, previous studies have noted that reduced gray matter volume is associated with increased structural covariance for such regions (Alexander-Bloch et al., 2013; Seeley et al., 2009). Our results suggest that in FM, the medial prefrontal/orbitofrontal cortex loses connections with other neighboring frontal regions, and instead gains connections with the cerebellum. While there is lack of evidence of direct anatomical connections between medial orbitofrontal cortex and pontine nuclei, a gateway to the cerebellum (Schmahmann, 1996), there is some evidence of polysynaptic functional connectivity. Human fMRI connectivity studies have demonstrated connectivity between medial frontal cortical areas and cerebellar lobules, while animal studies have demonstrated that cerebellar stimulation could modulate medial prefrontal activation via dopamine release in the ventral tegmental area (Habas et al., 2009; Krienen and Buckner, 2009; Rogers et al., 2011). Additionally, functional studies have noted that activity in both the orbitofrontal cortex and cerebellum are involved in pain relief (Leknes et al., 2011; Ploghaus et al., 1999), further supporting the importance of cerebellar activity and linking cerebellar and prefrontal cortical regions in pain modulation. Interestingly, pain experience and relief are known to be associated with reward processing (Seymour et al., 2005), and a study from our group has noted that fibromyalgia patients demonstrate disrupted reward-related circuitry (Loggia et al., 2014). In fact, previous neuroimaging studies have revealed generalized dysfunction in the reward/punishment-related circuitry and mesolimbic dopaminergic system in chronic pain patients (Baliki et al., 2012; Borsook et al., 2007; Loggia et al., 2014). Our findings of rich connections between the medial orbitofrontal cortex and cerebellum in FM, and the submodular association with depressive symptomatology and hyperalgesia in these patients, as identified by exploratory follow-up analyses, may also relate to abnormal reward processing in FM and chronic pain patients in general.

Altered structural covariance in FM also plays a role in clinically-relevant dysfunction in these patients. Specifically, we correlated the gray matter volume of the previously noted spectral partitioning submodules with clinical/behavioral measures and found that submodule 1 volume showed significant positive association with depression severity (i.e. BDI, Fig. 4). FM is known to be associated with significant depression and catastrophizing (Clauw, 2014), while chronic pain and depression are highly comorbid and show evidence of overlapping brain circuitry (Borsook et al., 2007). In chronic pain patients, BDI likely reflects affective aspects of somatic symptoms (Fishbain et al., 1997; Williams and Richardson, 1993), and the submodule 1 includes brain areas with relevance to affective processing. For instance, medial temporal lobe and cerebellum support affective aspects of evoked pain processing (Ploghaus et al., 1999; Ploghaus et al., 2001), and in chronic pain patients, the submodule 1 volume may play a role in affective dysfunction. Furthermore, submodule 2 volume was correlated with evoked pain sensitivity — reduced volume was associated with hyperalgesia (i.e. lower cuff pressure to elicit percept-matched 40/100 pain report). The submodule 2 includes primary somatosensory cortex and insula, areas known to support evoked pain intensity ratings in previous functional studies (Coghill

et al., 1999; Timmermann et al., 2001). As noted above, pain sensitivity did not show a significant correlation with BDI in FM patients. Moreover, clinical dysfunction (worse BDI, reduced pressure to evoke P40 pain) was associated with greater gray matter volume in submodule 1, but reduced volume in submodule 2. This differential association further underscores the independence of these different clinical aspects of fibromyalgia (i.e. depressive symptomatology and evoked pain hyperalgesia) and may have also contributed to, or resulted from, the differential spectral partitioning to these unique submodules within the FM structural covariance network. Notably, the gray matter volumes of submodules 1 and 2 both showed significant positive correlations with disease duration, which likely reflects the importance of pain chronicity in the structural neuroplasticity for these pain- and depression-related submodules in fibromyalgia patients.

As gray matter structural covariance was found to be altered in FM, we further hypothesized that white matter tracts connecting regions with altered covariance would also relate to clinically-relevant metrics in FM, and conducted exploratory follow-up analyses. Previous DTI studies revealed altered white matter morphometry in the corticospinal tract, as well as tracts leading from frontal, insular, and somatosensory cortices in chronic pain patients (Frøkjær et al., 2011; Geha et al., 2008; Lutz et al., 2008; Maeda et al., 2013). In our study, the submodule 1 included medial prefrontal/orbitofrontal cortex, medial temporal lobe, right inferior parietal lobule, and cerebellum clusters, which are connected by several white matter tracts such as the corticopontine tract, cerebellar peduncle, and uncinate fasciculus. We used probabilistic tractography and found that the number of estimated fibers in several tracts were associated with pain metrics (Fig. 5). For instance, the number of fiber tracts estimated by between cerebellum and both medial temporal lobe and inferior parietal lobule (supramarginal gyri and secondary somatosensory cortex) was negatively correlated with evoked pain sensitivity at P40 (i.e. stimulus pressure needed to achieve a pain rating of 40/100). Furthermore, the number of fiber tracts between medial temporal lobe and medial orbitofrontal lobe was correlated with clinical pain interference (BPI interference, a measure of pain-related quality of life). Thus, taken together, greater pain related dysfunction (i.e. greater pain interference, greater depression load, and worse evoked pain hyperalgesia) was associated with greater gray matter volume and white matter density (number of fibers within constituent tracts) for the submodule 1. Affective dysfunction is an important component of all of these pain-related metrics and previous studies have highlighted the medial orbitofrontal cortex, medial temporal lobe, inferior parietal lobule, and cerebellum in the processing of affective aspects of nociceptive afference (Borsook et al., 2007; Ploghaus et al., 1999; Wager et al., 2004). Our results extend our previous knowledge of the functional role for these brain regions and suggest that altered structural topology for corticocerebellar and frontotemporal connections may also be important to the pathophysiology of persistent chronic pain and co-morbid depression in FM.

Interestingly, submodule 1 in FM shares brain regions (e.g. inferior parietal lobule, medial prefrontal cortex, medial temporal lobe) previously attributed to the default mode network in functional MRI studies (Buckner et al., 2008; Greicius et al., 2003). Previous functional brain connectivity studies by our team have demonstrated that default mode network connectivity is associated with clinical pain (e.g. Loggia et al., 2011; Napadow et al., 2010; Napadow et al., 2012; Napadow and Harris, 2014). Our result from exploratory analyses demonstrated that gray matter volume in these regions was associated with BDI, while the number of white matter fibers connecting these regions was also associated with clinical pain, suggesting that structural change in the default mode network may underlie or be linked with pain-altered functional connectivity in these patients.

Some limitations to our study should be noted. Firstly, the structural covariance network analysis may be affected by the number or size of ROIs (Craddock et al., 2012; Hagmann et al., 2008). Also, network analysis based on anatomical ROI parcellation (e.g. AAL) may not accurately reflect functional connectivity features, which may bias network analysis (Craddock et al., 2012). However, it is important to note that our analysis focused on structural connectivity features and that a repeated structural covariance analysis using a significantly larger number of ROIs (531) also produced similar results. Secondly, we measured the strength of white matter connectivity using probabilistic tractography. While previous studies support links between tractograms obtained by computational methods and white-matter characterization by histology (Behrens et al., 2003; Ramnani et al., 2006), with corticopontocerebellar connections in specific being compared to data from invasive primate studies (Habas and Cabanis, 2007; Ramnani et al., 2006; Salmi et al., 2010), the tractogram is not a direct representation of nerve fiber tracts or axon tracing. However, only a small portion of cerebral peduncle fibers include corticospinal tract, and most pontine nuclei project to the cerebellum (Brodal, 1979; Ramnani et al., 2006). Thus, we can assume that the majority of tracts in the cerebral peduncle reach pontine nuclei, and continue on to the cerebellum via the middle cerebellar peduncle.

In summary, our structural covariance network analysis noted more dense connections in FM patients in the cerebellum, while healthy controls exhibited more dense frontal lobe connections. Spectral partitioning identified dense cerebellar connections to medial prefrontal/orbitofrontal cortex, medial temporal lobe, and right inferior parietal lobule in FM patients. These connections were merged into a distinct submodule 1, and the gray matter volume of this submodule was associated with the severity of depression symptoms in these patients. Additionally, analysis of white matter connectivity using probabilistic DTI methods demonstrated that the numbers of fibers between the submodule 1 regions were associated with greater evoked pain hyperalgesia and clinical pain interference. Hence, altered gray and white matter morphometry including cerebellar and frontal cortical regions may contribute to, or result from disrupted pain processing in chronic pain patients.

Conflicts of interest

Nothing to report.

Acknowledgements

This research was supported by National Center for Complementary and Alternative Medicine (P01-AT006663, R01-AT007550, R01-AR064367), National Institute of Arthritis and Musculoskeletal and Skin Diseases (R21-AR057920) and Korean Institute of Oriental Medicine (K15050). This research was made possible by the resources provided by Shared Instrumentation Grant (1S10RR023043).

Appendix A. Supplementary data

Supplementary material associated with this article can be found, in the online version, at http://dx.doi.org/doi:10.1016/j.nicl.2015.02.022.

References

Alexander-Bloch, A., Giedd, J.N., Bullmore, E., 2013. Imaging structural co-variance between human brain regions. Nat. Rev. Neurosci. 14 (5), 322–336. http://dx.doi.org/10.1038/nrn346523531697.

Ashburner, J., 2007. A fast diffeomorphic image registration algorithm. Neuroimage 38 (1), 95–113. http://dx.doi.org/10.1016/j.neuroimage.2007.07.00717761438.

Ashburner, J., Friston, K.J., 2005. Unified segmentation. Neuroimage 26 (3), 839–851. http://dx.doi.org/10.1016/j.neuroimage.2005.02.01815955494.

Baliki, M.N., Petre, B., Torbey, S., Herrmann, K.M., Huang, L., Schnitzer, T.J., Fields, H.L., Apkarian, A.V., 2012. Corticostriatal functional connectivity predicts transition to chronic back pain. Nat. Neurosci. 15 (8), 1117–1119. http://dx.doi.org/10.1038/nn.315322751038.

Baliki, M.N., Schnitzer, T.J., Bauer, W.R., Apkarian, A.V., 2011. Brain morphological signatures for chronic pain. P.L.O.S. ONE 6 (10), e26010. http://dx.doi.org/10.1371/journal.pone.002601022022493.

Bassett, D.S., Bullmore, E., Verchinski, B.A., Mattay, V.S., Weinberger, D.R., Meyer-Lindenberg, A., 2008. Hierarchical organization of human cortical networks in health and schizophrenia. J. Neurosci. 28 (37), 9239–9248. http://dx.doi.org/10.1523/JNEUROSCI.1929-08.200818784304.

Beck, A.T., Ward, C.H., Mendelson, M., Mock, J., Erbaugh, J., 1961. An inventory for measuring depression. Arch. Gen. Psychiatry 4, 561–571. http://dx.doi.org/10.1001/archpsyc.1961.01710120031004136883369.

Behrens, T.E., Berg, H.J., Jbabdi, S., Rushworth, M.F., Woolrich, M.W., 2007. Probabilistic diffusion tractography with multiple fibre orientations: what can we gain? Neuroimage 34 (1), 144–155. http://dx.doi.org/10.1016/j.neuroimage.2006.09.01817070705.

Behrens, T.E., Johansen-Berg, H., Woolrich, M.W., Smith, S.M., Wheeler-Kingshott, C.A., Boulby, P.A., Barker, G.J., Sillery, E.L., Sheehan, K., Ciccarelli, O., Thompson, A.J., Brady, J.M., Matthews, P.M., 2003. Non-invasive mapping of connections between human thalamus and cortex using diffusion imaging. Nat. Neurosci. 6 (7), 750–757. http://dx.doi.org/10.1038/nn107512808459.

Borsook, D., Becerra, L., Carlezon Jr., W.A., Shaw, M., Renshaw, P., Elman, I., Levine, J., 2007. Reward-aversion circuitry in analgesia and pain: implications for psychiatric disorders. Eur. J. Pain 11 (1), 7–20. http://dx.doi.org/10.1016/j.ejpain.2005.12.00516495096.

Brodal, P., 1979. The pontocerebellar projection in the rhesus monkey: an experimental study with retrograde axonal transport of horseradish peroxidase. Neurosci. 4 (2), 193–208. http://dx.doi.org/10.1016/0306-4522(79)90082-4106327.

Buckner, R.L., Andrews-Hanna, J.R., Schacter, D.L., 2008. The brain's default network: anatomy, function, and relevance to disease. Ann. N. Y. Acad. Sci. 1124, 1–38. http://dx.doi.org/10.1196/annals.1440.01118400922.

Bullmore, E., Sporns, O., 2009. Complex brain networks: graph theoretical analysis of structural and functional systems. Nat. Rev. Neurosci. 10 (3), 186–198. http://dx.doi.org/10.1038/nrn257519190637.

Chen, Z.J., He, Y., Rosa-Neto, P., Germann, J., Evans, A.C., 2008. Revealing modular architecture of human brain structural networks by using cortical thickness from MRI. Cereb. Cortex 18 (10), 2374–2381. http://dx.doi.org/10.1093/cercor/bhn00318267952.

Chi, J.G., Dooling, E.C., Gilles, F.H., 1977. Gyral development of the human brain. Ann. Neurol. 1 (1), 86–93. http://dx.doi.org/10.1002/ana.410010109560818.

Clauw, D.J., 2014. Fibromyalgia: a clinical review. JAMA 311 (15), 1547–1555. http://dx.doi.org/10.1001/jama.2014.326624737367.

Cleeland, C., 1991. Research in cancer pain. What we know and what we need to know. Cancer 67 (3 Suppl), 823–8271986852.

Coghill, R.C., Sang, C.N., Maisog, J.M., Iadarola, M.J., 1999. Pain intensity processing within the human brain: a bilateral, distributed mechanism. J. Neurophysiol. 82 (4), 1934–194310515983.

Craddock, R.C., James, G.A., Holtzheimer, P.E., Hu, X.P., Mayberg, H.S., 2012. A whole brain fMRI atlas generated via spatially constrained spectral clustering. Hum. Brain Mapp. 33 (8), 1914–1928. http://dx.doi.org/10.1002/hbm.2133321769991.

Evans, A.C., 2013. Networks of anatomical covariance. Neuroimage 80, 489–504. http://dx.doi.org/10.1016/j.neuroimage.2013.05.05423711536.

Fishbain, D.A., Cutler, R., Rosomoff, H.L., Rosomoff, R.S., 1997. Chronic pain-associated depression: antecedent or consequence of chronic pain? A review. Clin. J. Pain 13 (2), 116–137. http://dx.doi.org/10.1097/00002508-199706000-000069186019.

Ford, A., McGregor, K.M., Case, K., Crosson, B., White, K.D., 2010. Structural connectivity of Broca's area and medial frontal cortex. Neuroimage 52 (4), 1230–1237. http://dx.doi.org/10.1016/j.neuroimage.2010.05.01820488246.

Geha, P.Y., Baliki, M.N., Harden, R.N., Bauer, W.R., Parrish, T.B., Apkarian, A.V., 2008. The brain in chronic CRPS pain: abnormal gray-white matter interactions in emotional and autonomic regions. Neuron 60 (4), 570–581. http://dx.doi.org/10.1016/j.neuron.2008.08.02219038215.

Greicius, M.D., Krasnow, B., Reiss, A.L., Menon, V., 2003. Functional connectivity in the resting brain: a network analysis of the default mode hypothesis. Proc. Natl. Acad. Sci. U S A 100 (1), 253–258. http://dx.doi.org/10.1073/pnas.013505810012506194.

Habas, C., Cabanis, E.A., 2007. Anatomical parcellation of the brainstem and cerebellar white matter: a preliminary probabilistic tractography study at 3 T. Neuroradiol. 49 (10), 849–863. http://dx.doi.org/10.1007/s00234-007-0267-417701168.

Habas, C., Kamdar, N., Nguyen, D., Prater, K., Beckmann, C.F., Menon, V., Greicius, M.D., 2009. Distinct cerebellar contributions to intrinsic connectivity networks. J. Neurosci. 29 (26), 8586–8594. http://dx.doi.org/10.1523/JNEUROSCI.1868-09.200919571149.

Hagmann, P., Cammoun, L., Gigandet, X., Meuli, R., Honey, C.J., Wedeen, V.J., Sporns, O., 2008. Mapping the structural core of human cerebral cortex. P.L.O.S. Biol. 6 (7), e159. http://dx.doi.org/10.1371/journal.pbio.006015918597554.

Harris, R.E., Napadow, V., Huggins, J.P., Pauer, L., Kim, J., Hampson, J., Sundgren, P.C., Foerster, B., Petrou, M., Schmidt-Wilcke, T., Clauw, D.J., 2013. Pregabalin rectifies aberrant brain chemistry, connectivity, and functional response in chronic pain patients. Anesthesiology 119 (6), 1453–1464. http://dx.doi.org/10.1097/ALN.0000000000000001724343290.

He, Y., Chen, Z., Evans, A., 2008. Structural insights into aberrant topological patterns of large-scale cortical networks in Alzheimer's disease. J. Neurosci. 28 (18), 4756–4766. http://dx.doi.org/10.1523/JNEUROSCI.0141-08.200818448652.

He, Y., Chen, Z.J., Evans, A.C., 2007. Small-world anatomical networks in the human brain revealed by cortical thickness from MRI. Cereb. Cortex 17 (10), 2407–2419. http://dx.doi.org/10.1093/cercor/bhl14917204824.

Helmchen, C., Mohr, C., Erdmann, C., Petersen, D., Nitschke, M.F., 2003. Differential cerebellar activation related to perceived pain intensity during noxious thermal stimulation in humans: a functional magnetic resonance imaging study. Neurosci. Lett. 335 (3), 202–206. http://dx.doi.org/10.1016/S0304-3940(02)01164-312531467.

Jennrich, R.I., 1970. An asymptotic χ^2 test for the equality of two correlation matrices. J. Am. Stat. Assoc. 65 (330), 904–912. http://dx.doi.org/10.1080/01621459.1970.10481133.

Kim, J., Loggia, M.L., Cahalan, C., Harris, R.E., Beissner, F., Garcia, R., Kim, H.J., Wasan, A.D., Edwards, R.R., Napadow, V., The somatosensory link: S1 functional connectivity is altered by sustained pain and associated with clinical/autonomic dysfunction in fibromyalgia. Arthritis & Rheumatology (2015) in press [doi:10.1002/art.39043]

Kim, J., Loggia, M.L., Edwards, R.R., Wasan, A.D., Gollub, R.L., Napadow, V., 2013. Sustained deep-tissue pain alters functional brain connectivity. Pain 154 (8), 1343–1351. http://dx.doi.org/10.1016/j.pain.2013.04.01623718988.

Klein, A., Andersson, J., Ardekani, B.A., Ashburner, J., Avants, B., Chiang, M.C., Christensen, G.E., Collins, D.L., Gee, J., Hellier, P., Song, J.H., Jenkinson, M., Lepage, C., Rueckert, D., Thompson, P., Vercauteren, T., Woods, R.P., Mann, J.J., Parsey, R.V., 2009. Evaluation of 14 nonlinear deformation algorithms applied to human brain MRI registration. Neuroimage 46 (3), 786–802. http://dx.doi.org/10.1016/j.neuroimage.2008.12.03719195496.

Klöppel, S., Draganski, B., Golding, C.V., Chu, C., Nagy, Z., Cook, P.A., Hicks, S.L., Kennard, C., Alexander, D.C., Parker, G.J., Tabrizi, S.J., Frackowiak, R.S., 2008. White matter connections reflect changes in voluntary-guided saccades in pre-symptomatic Huntington's disease. Brain J. Neurol. 131 (1), 196–204. http://dx.doi.org/10.1093/brain/awm27518056161.

Krienen, F.M., Buckner, R.L., 2009. Segregated fronto-cerebellar circuits revealed by intrinsic functional connectivity. Cereb. Cortex 19 (10), 2485–2497. http://dx.doi.org/10.1093/cercor/bhp13519592571.

Kuchinad, A., Schweinhardt, P., Seminowicz, D.A., Wood, P.B., Chizh, B.A., Bushnell, M.C., 2007. Accelerated brain gray matter loss in fibromyalgia patients: premature aging of the brain? J. Neurosci. 27 (15), 4004–4007. http://dx.doi.org/10.1523/JNEUROSCI.0098-07.200717428976.

Leknes, S., Lee, M., Berna, C., Andersson, J., Tracey, I., 2011. Relief as a reward: hedonic and neural responses to safety from pain. P.L.O.S. ONE 6 (4), e17870. http://dx.doi.org/10.1371/journal.pone.001787021490964.

Liu, J., Zhao, L., Li, G., Xiong, S., Nan, J., Li, J., Yuan, K., von Deneen, K.M., Liang, F., Qin, W., Tian, J., 2012. Hierarchical alteration of brain structural and functional networks in female migraine sufferers. P.L.O.S. ONE 7 (12), e51250. http://dx.doi.org/10.1371/journal.pone.005125023227257.

Loggia, M.L., Berna, C., Kim, J., Cahalan, C.M., Gollub, R.L., Wasan, A.D., Harris, R.E., Edwards, R.R., Napadow, V., 2014. Disrupted brain circuitry for pain-related reward/punishment in fibromyalgia. Arthritis & Rheumatology (Hoboken, N.J.) 66 (1), 203–212. http://dx.doi.org/10.1002/art.3819124449585.

Loggia, M.L., Jensen, K., Gollub, R.L., Wasan, A.D., Edwards, R.R., Kong, J., 2011. The catechol-O-methyltransferase (COMT) val158met polymorphism affects brain responses to repeated painful stimuli. P.L.O.S. ONE 6 (11), e27764. http://dx.doi.org/10.1371/journal.pone.002776422132136.

Lutz, J., Jäger, L., de Quervain, D., Krauseneck, T., Padberg, F., Wichnalek, M., Beyer, A., Stahl, R., Zirngibl, B., Morhard, D., Reiser, M., Schelling, G., 2008. White and gray matter abnormalities in the brain of patients with fibromyalgia: a diffusion-tensor and volumetric imaging study. Arthritis Rheum. 58 (12), 3960–3969. http://dx.doi.org/10.1002/art.2407019035484.

Maeda, Y., Kettner, N., Sheehan, J., Kim, J., Cina, S., Malatesta, C., Gerber, J., McManus, C., Mezzacappa, P., Morse, L.R., Audette, J., Napadow, V., 2013. Altered brain morphometry in carpal tunnel syndrome is associated with median nerve pathology. Neuroimage. Clinical 2, 313–319. http://dx.doi.org/10.1016/j.nicl.2013.02.00123799199.

Mechelli, A., Friston, K.J., Frackowiak, R.S., Price, C.J., 2005. Structural covariance in the human cortex. J. Neurosci. 25 (36), 8303–8310. http://dx.doi.org/10.1523/JNEUROSCI.0357-05.200516148238.

Moulton, E.A., Schmahmann, J.D., Becerra, L., Borsook, D., 2010. The cerebellum and pain: passive integrator or active participator? Brain Res. Rev. 65 (1), 14–27. http://dx.doi.org/10.1016/j.brainresrev.2010.05.00520553761.

Mower, G., Gibson, A., Robinson, F., Stein, J., Glickstein, M., 1980. Visual pontocerebellar projections in the cat. J. Neurophysiol. 43 (2), 355–3667381525.

Napadow, V., Harris, R.E., 2014. What has functional connectivity and chemical neuroimaging in fibromyalgia taught us about the mechanisms and management of 'central-ized' pain? Arthritis Res. Ther. 16 (5), 425. http://dx.doi.org/10.1186/s13075-014-0425-025606591.

Napadow, V., Kim, J., Clauw, D.J., Harris, R.E., 2012. Decreased intrinsic brain connectivity is associated with reduced clinical pain in fibromyalgia. Arthritis Rheum. 64 (7), 2398–2403. http://dx.doi.org/10.1002/art.3441222294427.

Napadow, V., LaCount, L., Park, K., As-Sanie, S., Clauw, D.J., Harris, R.E., 2010. Intrinsic brain connectivity in fibromyalgia is associated with chronic pain intensity. Arthritis Rheum. 62 (8), 2545–2555. http://dx.doi.org/10.1002/art.2749720506181.

Newman, M.E.J., 2006. Modularity and community structure in networks. Proceedings of the National Academy of Sciences 103, 8577–8582. http://dx.doi.org/10.1073/pnas.0601602103.

Nosarti, C., Mechelli, A., Herrera, A., Walshe, M., Shergill, S.S., Murray, R.M., Rifkin, L., Allin, M.P., 2011. Structural covariance in the cortex of very preterm adolescents: a voxel-based morphometry study. Hum. Brain Mapp. 32 (10), 1615–1625. http://dx.doi.org/10.1002/hbm.2113320853378.

Ploghaus, A., Narain, C., Beckmann, C.F., Clare, S., Bantick, S., Wise, R., Matthews, P.M., Rawlins, J.N., Tracey, I., 2001. Exacerbation of pain by anxiety is associated with activity in a hippocampal network. J. Neurosci. 21 (24), 9896–990311739597.

Ploghaus, A., Tracey, I., Gati, J.S., Clare, S., Menon, R.S., Matthews, P.M., Rawlins, J.N., 1999. Dissociating pain from its anticipation in the human brain. Science 284 (5422), 1979–1981. http://dx.doi.org/10.1126/science.284.5422.197910373114.

Polianskis, R., Graven-Nielsen, T., Arendt-Nielsen, L., 2002. Pressure-pain function in desensitized and hypersensitized muscle and skin assessed by cuff algometry. J Pain 3 (1), 28–37. http://dx.doi.org/10.1054/jpai.2002.2714014622851.

Ramnani, N., Behrens, T.E., Johansen-Berg, H., Richter, M.C., Pinsk, M.A., Andersson, J.L., Rudebeck, P., Ciccarelli, O., Richter, W., Thompson, A.J., Gross, C.G., Robson, M.D., Kastner, S., Matthews, P.M., 2006. The evolution of prefrontal inputs to the cortico-pontine system: diffusion imaging evidence from macaque monkeys and humans. Cereb. Cortex 16 (6), 811–818. http://dx.doi.org/10.1093/cercor/bhj02416120793.

Rogers, T.D., Dickson, P.E., Heck, D.H., Goldowitz, D., Mittleman, G., Blaha, C.D., 2011. Connecting the dots of the cerebro-cerebellar role in cognitive function: neuronal pathways for cerebellar modulation of dopamine release in the prefrontal cortex. Synapse 65 (11), 1204–1212. http://dx.doi.org/10.1002/syn.2096021638338.

Salmi, J., Pallesen, K.J., Neuvonen, T., Brattico, E., Korvenoja, A., Salonen, O., Carlson, S., 2010. Cognitive and motor loops of the human cerebro-cerebellar system. J. Cogn. Neurosci. 22 (11), 2663–2676. http://dx.doi.org/10.1162/jocn.2009.2138219925191.

Schmahmann, J.D., 1996. From movement to thought: anatomic substrates of the cerebellar contribution to cognitive processing. Hum. Brain Mapp. 4 (3), 174–198. http://dx.doi.org/10.1002/(SICI)1097-0193(1996)4:3<174::AID-HBM3>3.0.CO;2-020408197.

Schmahmann, J.D., Doyon, J., McDonald, D., Holmes, C., Lavoie, K., Hurwitz, A.S., Kabani, N., Toga, A., Evans, A., Petrides, M., 1999. Three-dimensional MRI atlas of the human cerebellum in proportional stereotaxic space. Neuroimage 10 (3 1), 233–260. http://dx.doi.org/10.1006/nimg.1999.045910458940.

Schmidt-Wilcke, T., Luerding, R., Weigand, T., Jürgens, T., Schuierer, G., Leinisch, E., Bogdahn, U., 2007. Striatal grey matter increase in patients suffering from fibromyalgia — a voxel-based morphometry study. Pain 132 (Suppl. 1), S109–S116. http://dx.doi.org/10.1016/j.pain.2007.05.01017587497.

Seeley, W.W., Crawford, R.K., Zhou, J., Miller, B.L., Greicius, M.D., 2009. Neurodegenerative diseases target large-scale human brain networks. Neuron 62 (1), 42–52. http://dx.doi.org/10.1016/j.neuron.2009.03.02419376066.

Seymour, B., O'Doherty, J.P., Koltzenburg, M., Wiech, K., Frackowiak, R., Friston, K., Dolan, R., 2005. Opponent appetitive-aversive neural processes underlie predictive learning of pain relief. Nat. Neurosci. 8 (9), 1234–1240. http://dx.doi.org/10.1038/nn152716116445.

Smallwood, R.F., Laird, A.R., Ramage, A.E., Parkinson, A.L., Lewis, J., Clauw, D.J., Williams, D.A., Schmidt-Wilcke, T., Farrell, M.J., Eickhoff, S.B., Robin, D.A., 2013. Structural brain anomalies and chronic pain: a quantitative meta-analysis of gray matter volume. J Pain 14 (7), 663–675. http://dx.doi.org/10.1016/j.jpain.2013.03.00123685185.

Frøkjær, J.B., Olesen, S.S., Gram, M., Yavarian, Y., Bouwense, S.A., Wilder-Smith, O.H., Drewes, A.M., 2011. Altered brain microstructure assessed by diffusion tensor imaging in patients with chronic pancreatitis. Gut 60 (11), 1554–1562. http://dx.doi.org/10.1136/gut.2010.23662021610272.

Timmermann, L., Ploner, M., Haucke, K., Schmitz, F., Baltissen, R., Schnitzler, A., 2001. Differential coding of pain intensity in the human primary and secondary somatosensory cortex. J. Neurophysiol. 86 (3), 1499–150311535693.

Tomassini, V., Jbabdi, S., Klein, J.C., Behrens, T.E., Pozzilli, C., Matthews, P.M., Rushworth, M.F., Johansen-Berg, H., 2007. Diffusion-weighted imaging tractography-based parcellation of the human lateral premotor cortex identifies dorsal and ventral subregions with anatomical and functional specializations. J. Neurosci. 27 (38), 10259–10269. http://dx.doi.org/10.1523/JNEUROSCI.2144-07.200717881532.

Tzourio-Mazoyer, N., Landeau, B., Papathanassiou, D., Crivello, F., Etard, O., Delcroix, N., Mazoyer, B., Joliot, M., 2002. Automated anatomical labeling of activations in SPM using a macroscopic anatomical parcellation of the MNI MRI single-subject brain. Neuroimage 15 (1), 273–289. http://dx.doi.org/10.1006/nimg.2001.097811771995.

Wager, T.D., Rilling, J.K., Smith, E.E., Sokolik, A., Casey, K.L., Davidson, R.J., Kosslyn, S.M., Rose, R.M., Cohen, J.D., 2004. Placebo-induced changes in fMRI in the anticipation and experience of pain. Science 303 (5661), 1162–1167. http://dx.doi.org/10.1126/science.109306514976306.

Williams, A.C., Richardson, P.H., 1993. What does the BDI measure in chronic pain? Pain 55 (2), 259–266. http://dx.doi.org/10.1016/0304-3959(93)90155-I8309713.

Wolfe, F., Clauw, D.J., Fitzcharles, M.A., Goldenberg, D.L., Katz, R.S., Mease, P., Russell, A.S., Russell, I.J., Winfield, J.B., Yunus, M.B., 2010. The American College of Rheumatology preliminary diagnostic criteria for fibromyalgia and measurement of symptom severity. Arthritis Care Res. 62 (5), 600–610. http://dx.doi.org/10.1002/acr.2014020461783.

Woolrich, M.W., Jbabdi, S., Patenaude, B., Chappell, M., Makni, S., Behrens, T., Beckmann, C., Jenkinson, M., Smith, S.M., 2009. Bayesian analysis of neuroimaging data in FSL. Neuroimage 45 (1), S173–S186.